Mapping the principal gradient onto the corpus callosum

Patrick Friedrich [a, b,*], Stephanie J. Forkel[a, b, c], and Michel Thiebaut de Schotten [a, b]

[a] *Brain Connectivity and Behaviour Laboratory, Sorbonne Universities, Paris, France.*

[b] *Groupe d'Imagerie Neurofonctionnelle, Institut des Maladies Neurodégénératives-UMR 5293, CNRS, CEA University of Bordeaux, Bordeaux, France.*

[c] *Centre for Neuroimaging Sciences, Department of Neuroimaging, Institute of Psychiatry, Psychology and Neuroscience, King's College London, London, UK.*

* Corresponding author: patrick.friedrich@rub.de

Abstract

Gradients capture some of the variance of the resting-state functional magnetic resonance imaging (rsfMRI) signal. Amongst these, the principal gradient depicts a functional processing hierarchy that spans from sensory-motor cortices to regions of the default-mode network. While the cortex has been well characterised in terms of gradients little is known about its underlying white matter. For instance, comprehensive mapping of the principal gradient on the largest white matter tract, the corpus callosum, is still missing. We hence mapped the principal gradient onto the callosal midsection using the 7T human connectome project dataset. We further explored how quantitative measures and variability in callosal midsection connectivity relate to the principal gradient values. In so doing, we demonstrated that the extreme values of the principal gradient are located within the callosal genu and the posterior body, have lower connectivity variability but a larger spatial extent along the midsection of the corpus callosum than mid-range values. Our results shed light on the relationship between the brain's functional hierarchy and the corpus callosum. We further speculate about how these results may bridge the gap between functional hierarchy, brain asymmetries, and evolution.

Introduction

Cognitive neurosciences assume that cognition is embedded within and constraint by the organization of the brain. The advent of neuroimaging methods granted novel insights into the functional organization of the living human brain. Resting-state functional connectivity (rsfMRI), in particular, has proven useful for mapping multiple functional networks without relying on participants to perform functional tasks in the scanner (Smith et al., 2009; Power et al., 2011; Biswal et al., 1995). rsfMRI networks reveal different time courses and spatially correspond to tasks-related functional activations (Tavor et al., 2016). This spatial correspondence suggests an underlying organization that adheres to fundamental principles. For instance, Mesulam (1998) proposes that brain regions can be organised along a gradient ranging from sensory-motor to higher-order brain processes. In line with Mesulam, most of the variance of rsfMRI resembles a gradient that spans from sensory-motor cortices to regions of the default-mode network (i.e. latter is referred to as the principal gradient, Margulies et al., 2016). While, sensory-motor cortices are primary cortices (i.e. idiotypic areas Mesulam, 1998) and the default-mode network has been associated with transmodal higher-order functions (Margulies et al., 2016, Alves et al. 2019). The principal gradient may thus represent one fundamental principle driving a hierarchical organisation of cognitive functions (Huntenburg, Bazin, & Margulies, 2018).

While this principal gradient is putatively the same for both hemispheres (Margulies et al., 2016) little is known on the connections between the left and the right principal gradient. With 200 to 300 millions axons (Tomasch 1954), the largest white matter commissure in the primate brain is the corpus callosum (Burdach 1826). While other routes of interhemispheric interactions are possible (e.g. anterior commissure, Risse et al., 1978), surgically severing callosal connections severaly interrupts interhemispheric functional connectivity in monkeys (Johnston et al., 2008; O'Reilly et al. 2013) and humans (Roland et al., 2017). Concordantly, studies in split-brain patients present with severe behavioral manifestations such as Alien hand syndrome (Akelaitis 1945; Bogen, 1993) Hemispatial Neglect (Kashiwagi *et al.*, 1990; Heilman and Adams, 2003; Lausberg *et al.*, 2003; Park *et al.*, 2006; Tomaiuolo *et al.*, 2010) Optic aphasia (Freund, 1889; Luzzatti *et al.*, 1998) or pure alexia (Dejerine, 1892; Geschwind and Fusillo, 1966) amongst others. The corpus callosum is hence considered critical for the collaborative integration of functions relying on both hemispheres. Despite its crucial role, current parcellation approaches have only segregated the corpus callosum based on its cytoarchitecture, geometry and topological projections.

Several methods have been proposed to parcellate or segment the corpus callosum. Amongst these methods, four main classifications are still currently applied. Post mortem studies identified anatomical features along the midsagittal section of the corpus callosum, including the rostrum, genu, anterior and posterior body, isthmus and splenium (Crosby et al., 1962 ; figure 1A). While this classification is still widely used today, it does not define clear boundaries between the different segments. A second tentatively sharper parcellation was based on histological measures of the midsagittal axonal diameter but it fails to systematically generalise across individuals (Aboitiz & Montiel, 2003, 1992, figure 1B). The enforcement of a geometrical grid of seven parcels has been used to somewhat circumvent the limitations of generalisation (Wittelson, 1989; figure 1C). All these anatomical, histological and geometrical parcellations of the midsection of the corpus callosum do however not consider the functional organisation of the brain it connects.

Since the functions of the corpus callosum are defined by the areas that it connects to, tract-tracing in non-human primates (Schmahmann and Pandya 2009) or diffusion weighted imaging tractography in humans (Huang et al., 2005; Hofer and Frahm, 2006, figure 1D), is likely the most promising appraoch to investigate the functional organisation of the corpus callosum. However, a comprehensive mapping of the hierarchical organisation of cognitive functions on the corpus callosum is still missing.

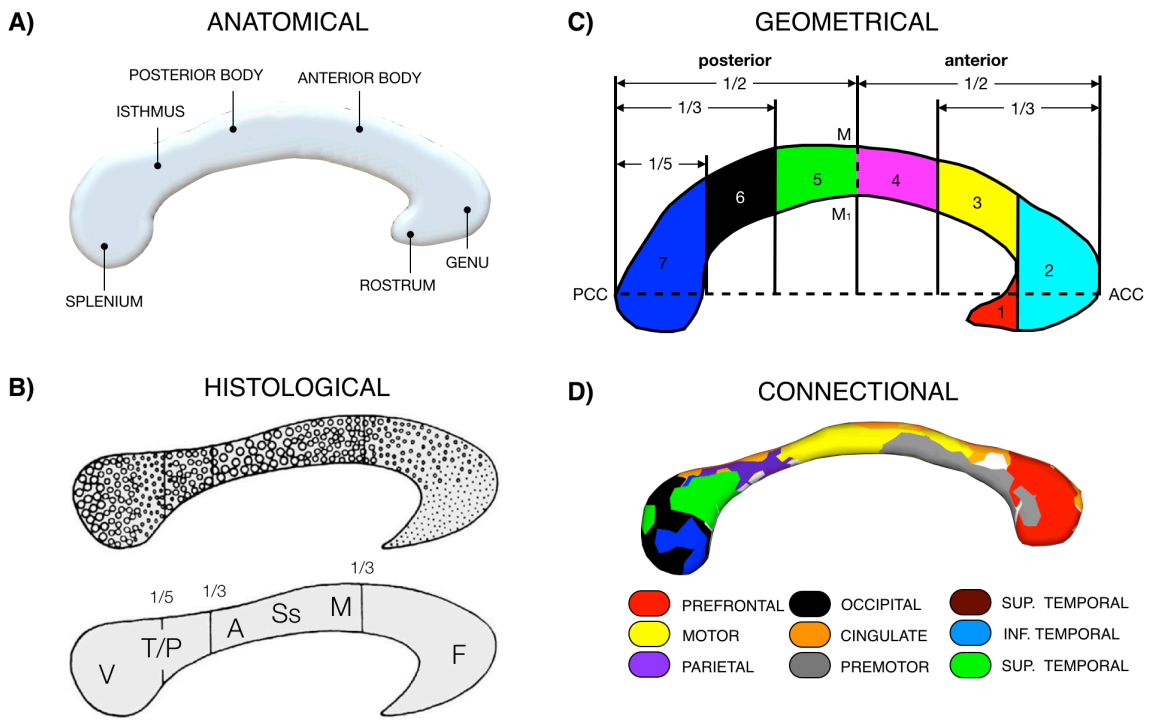

Figure 1. Parcellations of the corpus callosum along the midsection (right view). A) Anatomical

division: depicts the anatomical classification (rostrum, genu, anterior and posterior body, isthmus, splenium) based on gross anatomical features. B) Histological division: the dots in this schematic diagram indicate the range of axonal density and associate them with cortical projections to cortical areas (F: Frontal, M: Motor, SS: Somato-Sensory, A: Auditory, T/P: Temporo-Parietal and V: Visual (from Aboitiz & Montiel, 2003). C) Geometrical division: This parcellation generates seven parcels by equally diving the midsection (from Wittelson, 1989). ACC: most anterior point of the corpus callosum, PCC: most posterior point of the corpus callosum, M: middle of the corpus callosum. D: Connectional division: Shows the parcellation of the cortex based on diffusion tractography (from Catani & Thiebaut de Schotten 2012).

In this study we, therefore, propose a novel division of the corpus callosum based on the projection of the principal gradient onto the callosal midsection. We also explored how variability in connectivity and quantitative measures of this connectivity relate to the principal gradient values along the callosal midsection.

Methods

Dataset

All 7T rsfMRI and diffusion-weighted data used in this study were provided within the Human Connectome Project (HCP; Van Essen et al, 2013) which is publicly available and anonymized. Participant recruitment procedures and informed consent forms, including consent to share de-identified data, were previously approved by the Washington University Institutional Review Board.

Gradient percentile maps

We used an averaged map of the principal gradient published elsewhere (Margulies et al., 2016, see figure 2A). In Margulies et al. (2016), functional connectivity matrices were calculated from the HCP dataset and the gradient extracted using nonlinear dimensionality reduction via diffusion embedding (Coifman et al., 2005). In order to assess callosal connections to cortical regions along the principal gradient, we segregated voxels within the cortex based on their location along the principal gradient. We parcellated the principal gradient map into 100 units where each unit represents one percentile of the principal gradient. All operations were conducted using FSL (www.fmrib.ox.ac.uk/fsl). The gradient intensities range between -7.52 and +10.07. A central value of 0 denoted areas not defined

along the gradient. For computational reasons, we transposed the gradient values by multiplying the minimum intensity value by -1. We subsequently masked the results with a binarized map of the principal gradient. The resulting image was masked with a cortical grey matter template (i.e. Fast applied to MNI152 template). This resulted in 100 distinct gradient percentile maps, each one presenting a 1% range of the gradient (see figure 2B).

Mapping the principal gradient onto the corpus callosum.

In order to map the gradient along the white mater connections, we employed the Disconnectome within the BCBtoolkit (Foulon et al. 2018) using a study-specific HCP dataset of 163 participants to generate the underlying white matter tractograms (Karolis et al. 2019). For each gradient percentile map, the Disconnectome filtered tractography of the white matter tractograms. The resulting filtered tractography was transformed into visitation maps (i.e. binary mask of the voxels including more that 1 streamline, Thiebaut de Schotten et al., 2011). To generate a group-level visitation map, all normalised individual visitation maps were averaged voxel-by-voxel. This group-level visitation map represents the connection probability per voxel, and thus accounts for the interindividual variability of the anatomical representation of tracts for the respective gradient percentile map (see Figure 2C). All visitation maps are in MNI152 space and are available upon request to the corresponding author.

This study focussed on the relationship between the functional gradient and the interhemispheric commissural connections of the corpus callosum. We manually delineated the corpus callosum midsection on the midsagittal slice of the MNI152 template. For each gradient percentile, the visitation map was masked with the corpus callosum midsection to reconstruct callosal connectivity maps (see figure 2D). We subsequently created a weighted average map based on the following equation, in which the callosal connectivity maps were divided by the sum of all callosal connectivity maps.

$$weighted\ average\ connectivity\ map\ =\ \Sigma\ ((\frac{connectivity\ map}{\Sigma\ connectivity\ maps}) * gradient\ percentile)\ /\ 100$$

Each of the divided visitation maps was then multiplied by the respective level of the gradient (1% = times 1, 2% = times 2, etc.). This resulted in 100 weighted callosal connectivity maps, one for each gradient percentile. To obtain one single unified callosal connectivity gradient map, the weighted connectome maps were summed up and divided by the number of percentiles (n=100). The resulting weighted average connectivity map is shown in Figure 2E.

Statistical analyses

Statistical analyses were performed in SPSS (IBM SPSS Statistics, Version 24.0. Armonk, NY: IBM Corp.). In order to avoid spurious measurements, we truncated the distribution of the gradient percentile maps at either end to avoid including maps with less than 300 voxels (supplementary figure 1). Included percentile maps ranged from 13% to 82% (equivalent original gradient values: –5.23 to +6.90). We explored how variability in connectivity and quantitative measures of callosal connectivity relates to the principal gradient values. The connectivity probability between the corpus callosum and the gradient percentile was calculated by averaging each callosal connectivity map. The callosal space occupied by each percentile was defined as the number of non-zero voxels for each callosal connectivity map. To explore the relationship between the corpus callosum and the principal gradient, we plotted the connection probability against the residuals of the gradient value and the number of voxels of the respective gradient percentile map. We chose to correct the gradient values in this analysis for the number of voxels in the respective gradient percentile map as more voxels will invariably lead to higher level of connection probability. The same procedure was applied to plot the callosal space occupied by each percentile. The two distributions were visually inspected and scrutinised with either linear or quadratic regression as applicable.

Results

Corpus callosum gradient map

The principal gradient projections on the corpus callosum is displayed below (Figure 2E).

Results indicate a structured distribution of the principal gradient along the midsection of the corpus callosum where the anterior corpus callosum is more likely connected to areas of higher principal gradient values compared to posterior areas. Accordingly, the negative spectrum of the principal gradient peaked in the isthmus and the posterior body, whereas the positive spectrum occupied the anterior part of the body, the genu and the rostrum. In some parts of the splenium a small peak of positive values was also evident.

Relationship between the principal gradient and callosal connectivity

Visual inspection of the data clearly indicated a U-shaped distribution. Using a curve-fit estimation, we investigated the possibility for either a linear or quadratic relationship between connection probability and the principal gradient. A linear regression model was fitted onto the distribution (Y_i = 0.229 + -0.002*X_i), which did not match the data ($F_{(1, 68)}$ = 0.698, r^2 = 0.010, p = 0.406). However, a quadratic regression revealed a highly significant (r^2 = 0.739, p < 0.001) relationship (Y_i = 0.174 + -0.006*X_i + 0.004*X^2_i) between callosal connection probability and the principal gradient as illustrated in Figure 2F.

Relationship between the principal gradient and associated callosal area

Similar to the previous analysis, a curve-fit estimation was employed to investigate a linear or quadratic relationship between the number of callosal voxels that may connect to a certain gradient value. A linear regression model (Y_i = 840.029 + 5.280*X_i) failed to reach significance ($F_{(1,68)}$ = 3.147, r^2 = 0.044, p = 0.081), while the quadratic model reached significance (Y_i = 906.792 + 10.801*X_i + -5.387*X^2_i with $F_{(2,67)}$ = 41.708, r^2 = 0.555, p < 0.001). The inverted U-shaped distribution of associated callosal areas across the principal gradient is depicted below (Figure 2F).

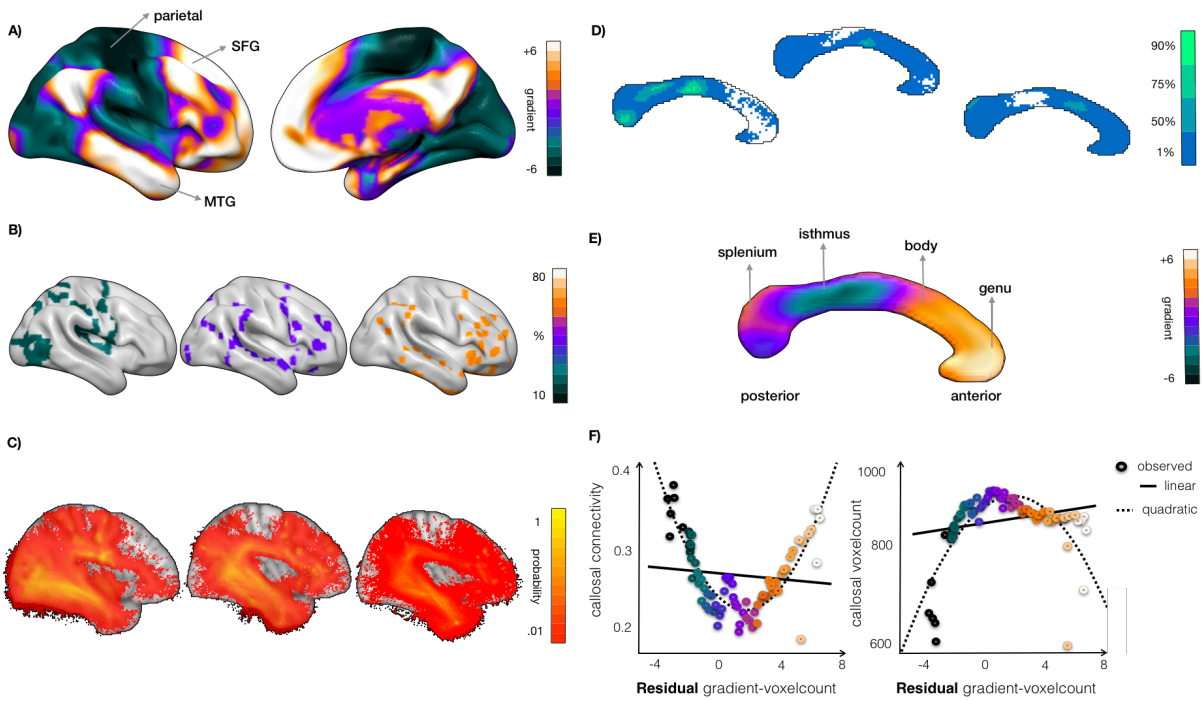

Figure 2. Mapping the principal gradient on the corpus callosum. A) Visualisation of the principal gradient on the cortical surface. B) Examples for percentile maps (20-40-60%) depicting associated

cortical areas. C) Percentile-specific tractograms as derived from the percentile gradients maps shown in B). D) Midsagittal display of the thresholds for callosal connectivity based on the tractograms for the 20th, 40th and 60th gradient percentiles. The lower the threshold the less participants showed callosal connections in this voxel. E) presents the callosal gradient map which was computed as the voxel-wise weighted average of callosal connectivity across all percentile maps of the gradient. F) scatterplots showing the relation between averaged callosal connectivity (left) or number of non-zero connectivity voxels (right) and the residual between the gradient corrected for the number of voxels in the respective gradient percentile map.

Discussion

The current study investigated the relationship between the principal gradient and cortical projections of the corpus callosum. We reveal three main results: First, the apexes of the principal gradient span from the genu to the posterior body. Second, the individual variability of callosal connectivity is lowest at the apexes of the gradient. Lastly, the number of connected voxels in the callosal midsection was the smallest for the apexes of the gradient. These results shed light onto the evolutionary processes involved into interhemispheric communication.

To depict the principal gradient on the callosal midsection, we mapped each percentile of the gradient independently. The callosal gradient (Figure 2E) indicates that the negative spectrum of the principal gradient peaks in the posterior body, whereas the positive spectrum peaks in the genu. Previous research demonstrated that the posterior midbody contains fibers that project to lower-level processing areas (e.g. somatosensory areas; Schmahmann and Pandya 2009). The genu connects to higher-level associative regions (i.e. prefrontal and orbitofrontal cortices; Schmahmann and Pandya 2009). Hence the spatial layout of the callosal gradient map is concordant with a previously hypothesised anatomical-functional organisation of the corpus callosum (Catani & Thiebaut de Schotten 2012). Additionally, the callosal gradient resembles previous work mapping the diameter and myelination of callosal fibres (Aboitiz et al, 1992; Aboitiz & Montiel 2003). Accordingly, the genu contains poorly myelinated fibers of thin diameter compared to callosal fibers that connect to the posterior midbody. Diameter and myelination are contingent on conduction speed (Hursh, 1939; Waxman & Bennett, 1972). The callosal gradient, therefore, may encode a functional hierarchy with slow and fast conduction speeds for transmodal and unimodal processes.

This general principle demonstrated at the group level appears to hold on the individual level given that interindividual variability in callosal connectivity was lowest for the apexes of the gradient. This findings feeds into a recent hypothesis where structural variability is associated with evolutionary stability (Croxson, Forkel, & Thiebaut de Schotten, 2017). The observed callosal connectivity results may thus be linked to the phylogenetic age of cortical areas. Based on the dual origin theory, it has been suggested that multimodal, prefrontal and paralimbic cortices may have evolved in parallel to sensory and motor cortices (Pandy, Petrides, & Cipolloni, 2015). With regards to the gradient architecture, support for this assumption comes from non-human primate studies. For instance, a comparison between resting-state based gradients in human and structural connectivity-based gradients in macaque monkey displayed similar spatial layouts spanning from primary sensory-motor to fronto-parietal regions (Oligschläger et al, 2019). In humans, this transmodal end of the gradient concords with the default mode network that is also present in chimpanzees (Barks, Parr, and Rilling, 2013) and macaque monkeys (Mantini et al., 2011). Hence several pieces of evidence converge towards phylogenetic older apexes of the gradient. Additionally, the variability in callosal connectivity suggests a more symmetrical functional organization at the apexes of the gradient (Karolis, Corballis, and Thiebaut de Schotten, 2019). While these arguments may support the interpretation that callosal connectivity may be a proxy for evolutionary stability, comparative studies may compare the callosal gradient architecture across primate species and derive phylogenetic models in order to test this assumption.

A decrease in the variability of callocal connectivity at either end of the gradient was also accompanied by a decrease of the number of voxels connected in the callosal midsagittal area (Figure 2F, right side). Inversely, callosal connectivity was more variable and involved more voxels in the associated callosal area when distant from the gradient's apexes. According to the tethering hypothesis, evolutionary expansion of the human cortex may have untethered large portions of the cortex from the constraints of early sensory activation cascades and molecular gradients (Buckner & Krienen, 2013). Similarly, the dual origin suggests that evolution progressively expended two cortical trends, one of which emerges from the hippocampocentric division (Pandya et al. 2015) and forms the limbic system that is cortically represented by the default mode network (Alves et al. 2019). In other words, evolutionary expansion would have created regions less functionally restricted than the apexes of the gradient. This, in turn, could lead to a more diverse pattern of connectivity (i.e. higher number of voxels in the associated callosal area) which is in accordance with the observed higher individual variability and the tethering as well as the dual origin hypotheses.

Some limitation should be acknowledged in this study. While we describe the first corpus callosum principal gradient map, this map depicts the weighted average of structural connectivity, based on an averaged map of the principal gradient. The weighted average of structural connectivity allowed us to assess - to some extent- the variability of callosal connectivity, however, individual patterns of the principal gradient are yet unavailable. Therefore, the effect of individual variability of the principal gradient's spatial layout on callosal projections could not be assessed in this study. Addressing the extent to which the principal gradient and its callosal connections differ across individuals will be a matter of future research.

Conclusion

Our study provides the first comprehensive map of the callosal cross-section that displays the distribution of callosal connections according to a hierarchical organisation of cognitive functions. Our findings align with previous considerations about the evolutionary changes in the brain. Future studies may utilize the map of the callosal gradient to bridge the gap between brain asymmetries and functional hierarchy.

Acknowledgements

European Research Council (ERC) under the European Union's Horizon 2020 research and innovation programme (grant no. 818521)

References

Aboitiz, F., & Montiel, J. (2003). One hundred million years of interhemispheric communication: the history of the corpus callosum. *Brazilian journal of medical and biological research*, *36*(4), 409-420.

Akelaitis, A. J. (1945). Studies on the corpus callosum: IV. Diagonistic dyspraxia in epileptics following partial and complete section of the corpus callosum. *American Journal of Psychiatry*, *101*(5), 594-599.

Alves, P. N., Foulon, C., Karolis, V., Bzdok, D., Margulies, D. S., Volle, E., & de Schotten, M. T. (2019). An improved neuroanatomical model of the default-mode network reconciles previous neuroimaging and neuropathological findings. *Communications biology*, *2*(1), 1-14.

Barks, S. K., Parr, L. A., & Rilling, J. K. (2015). The default mode network in chimpanzees (Pan troglodytes) is similar to that of humans. *Cerebral cortex*, *25*(2), 538-544.

Biswal, B., Zerrin Yetkin, F., Haughton, V. M., & Hyde, J. S. (1995). Functional connectivity in the motor cortex of resting human brain using echo-planar MRI. *Magnetic resonance in medicine*, *34*(4), 537-541.

Bogen, J. E. (1993). The callosal syndromes. In K. M. Heilman & E. Valenstein (Eds.), Clinical neuropsychology (p. 337–407). Oxford University Press.

Buckner, R. L., & Krienen, F. M. (2013). The evolution of distributed association networks in the human brain. *Trends in cognitive sciences*, *17*(12), 648-665.

Burdach, K. F., & Royal College of Physicians of London. (1819). *Vom Baue und Leben des Gehirns*. (Medical Heritage Library.) Leipzig: Dy'sche Buchhandlung.

Catani, M., & de Schotten, M. T. (2012). *Atlas of human brain connections*. Oxford University Press.

Coifman, R. R., Lafon, S., Lee, A. B., Maggioni, M., Nadler, B., Warner, F., & Zucker, S. W. (2005). Geometric diffusions as a tool for harmonic analysis and structure definition of data: Diffusion maps. *Proceedings of the national academy of sciences*, *102*(21), 7426-7431.

Crosby, E. C., Humphrey, T., & Lauer, E. W. (1962). White matter of the hemisphere, Pt 3. *Correlative anatomy of the nervous system. New York: Macmillan*.

Croxson, P. L., Forkel, S. J., Cerliani, L., & Thiebaut de Schotten, M. (2018). Structural variability across the primate brain: a cross-species comparison. *Cerebral Cortex*, *28*(11), 3829-3841.

Dejerine, J. (1892). Contribution à l'étude anatomopathologique et clinique des différents variétés de cécité verbale. *Mémoires de la Société de Biologie*, *4*, 61-90.

Foulon, C., Cerliani, L., Kinkingnehun, S., Levy, R., Rosso, C., Urbanski, M., ... & Thiebaut de Schotten, M. (2018). Advanced lesion symptom mapping analyses and implementation as BCBtoolkit. *GigaScience*, *7*(3), giy004.

Freund, C. S. (1889). II. Heber optische Aphasie und Seelenblindheit. *Archiv für Psychiatrie und Nervenkrankheiten*, *20*(1), 276-297.

Geschwind, N., & Fusillo, M. (1966). Color-naming defects in association with alexia. *Archives of Neurology*, *15*(2), 137-146.

Heilman, K. M., & Adams, D. J. (2003). Callosal neglect. *Archives of neurology*, *60*(2), 276-279.

Hofer, S., & Frahm, J. (2006). Topography of the human corpus callosum revisited—comprehensive fiber tractography using diffusion tensor magnetic resonance imaging. *Neuroimage*, *32*(3), 989-994.

Huang, H., Zhang, J., Jiang, H., Wakana, S., Poetscher, L., Miller, M. I., ... & Mori, S. (2005). DTI tractography based parcellation of white matter: application to the mid-sagittal morphology of corpus callosum. *Neuroimage*, *26*(1), 195-205.

Huntenburg, J. M., Bazin, P. L., & Margulies, D. S. (2018). Large-scale gradients in human cortical organization. *Trends in cognitive sciences*, *22*(1), 21-31.

Hursh, J. B. (1939). Conduction velocity and diameter of nerve fibers. *American Journal of Physiology-Legacy Content*, *127*(1), 131-139.

Johnston, J. M., Vaishnavi, S. N., Smyth, M. D., Zhang, D., He, B. J., Zempel, J. M., ... & Raichle, M. E. (2008). Loss of resting interhemispheric functional connectivity after complete section of the corpus callosum. *Journal of Neuroscience*, *28*(25), 6453-6458.

Karolis, V. R., Corbetta, M., & De Schotten, M. T. (2019). The architecture of functional lateralisation and its relationship to callosal connectivity in the human brain. *Nature communications*, *10*(1), 1-9.

Kashiwagi A, Kashiwagi T, Nishikawa T, Tanabe H, Okuda J. 1990.Hemispatial neglect in a patient with callosal infarction. *Brain*, 113(4):1005-1023.

Lausberg, H., Kita, S., Zaidel, E., & Ptito, A. (2003). Split-brain patients neglect left personal space during right-handed gestures. *Neuropsychologia*, *41*(10), 1317-1329.

Luzzatti, C., Vecchi, T., Agazzi, D., Cesa-Bianchi, M., & Vergani, C. (1998). A neurological dissociation between preserved visual and impaired spatial processing in mental imagery. *Cortex*, *34*(3), 461-469.

Mantini, D., Gerits, A., Nelissen, K., Durand, J. B., Joly, O., Simone, L., ... & Vanduffel, W. (2011). Default mode of brain function in monkeys. *Journal of Neuroscience*, *31*(36), 12954-12962.

Margulies, D. S., Ghosh, S. S., Goulas, A., Falkiewicz, M., Huntenburg, J. M., Langs, G., ... & Jefferies, E. (2016). Situating the default-mode network along a principal gradient of macroscale cortical organization. *Proceedings of the National Academy of Sciences*, *113*(44), 12574-12579.

Mesulam, M. M. (1998). From sensation to cognition. *Brain: a journal of neurology*, *121*(6), 1013-1052.

Oligschläger, S., Xu, T., Baczkowski, B. M., Falkiewicz, M., Falchier, A., Linn, G., & Margulies, D. S. (2019). Gradients of connectivity distance in the cerebral cortex of the macaque monkey. *Brain Structure and Function*, *224*(2), 925-935.

O'Reilly, J. X., Croxson, P. L., Jbabdi, S., Sallet, J., Noonan, M. P., Mars, R. B., ... & Rushworth, M. F. (2013). Causal effect of disconnection lesions on interhemispheric functional connectivity in rhesus monkeys. *Proceedings of the National Academy of Sciences*, *110*(34), 13982-13987.

Pandya, D., Petrides, M., & Cipolloni, P. B. (2015). *Cerebral cortex: architecture, connections, and the dual origin concept*. Oxford University Press.

Park KC, Lee BH, Kim EJ, Shin MH, Choi KM, Yoon SS, Kwon SU, ChungCS, Lee KH, Heilman KM et al. 2006. Deafferentation-disconnection neglect induced by posterior cerebral artery infarction. Neurology.66(1):56-61.

Power, J. D., Cohen, A. L., Nelson, S. M., Wig, G. S., Barnes, K. A., Church, J. A., ... & Petersen, S. E. (2011). Functional network organization of the human brain. *Neuron*, *72*(4), 665-678.

Risse, G. L., LeDoux, J., Springer, S. P., Wilson, D. H., & Gazzaniga, M. S. (1978). The anterior commissure in man: Functional variation in a multisensory system. *Neuropsychologia*, *16*(1), 23-31.

Roland, J. L., Snyder, A. Z., Hacker, C. D., Mitra, A., Shimony, J. S., Limbrick, D. D., ... & Leuthardt, E. C. (2017). On the role of the corpus callosum in interhemispheric functional connectivity in humans. *Proceedings of the National Academy of Sciences*, *114*(50), 13278-13283.

Schmahmann, J. D., Schmahmann, J., & Pandya, D. (2009). *Fiber pathways of the brain*. OUP USA.

Smith, S. M., Fox, P. T., Miller, K. L., Glahn, D. C., Fox, P. M., Mackay, C. E., ... & Beckmann, C. F. (2009). Correspondence of the brain's functional architecture during activation and rest. *Proceedings of the National Academy of Sciences*, *106*(31), 13040-13045.

Tavor, I., Jones, O. P., Mars, R. B., Smith, S. M., Behrens, T. E., & Jbabdi, S. (2016). Task-free MRI predicts individual differences in brain activity during task performance. *Science*, *352*(6282), 216-220.

Thiebaut de Schotten, M., Bizzi, A., Dell'Acqua, F., Allin, M., Walshe, M., Murray, R., ... & Catani, M. (2011). Atlasing location, asymmetry and inter-subject variability of white matter tracts in the human brain with MR diffusion tractography. *Neuroimage*, *54*(1), 49-59.

Tomaiuolo, F., Voci, L., Bresci, M., Cozza, S., Posteraro, F., Oliva, M., & Doricchi, F. (2010). Selective visual neglect in right brain damaged patients with splenial interhemispheric disconnection. *Experimental brain research*, *206*(2), 209-217.

Tomasch, J. (1954). Size, distribution, and number of fibres in the human corpus callosum. *The Anatomical Record*, *119*(1), 119-135.

Van Essen, D. C., Smith, S. M., Barch, D. M., Behrens, T. E., Yacoub, E., Ugurbil, K., & Wu-Minn HCP Consortium. (2013). The WU-Minn human connectome project: an overview. *Neuroimage*, *80*, 62-79.

Waxman, S. G., & Bennett, M. V. (1972). Relative conduction velocities of small myelinated and non-myelinated fibres in the central nervous system. *Nature New Biology*, *238*(85), 217-219.

Witelson, S. F. (1989). Hand and sex differences in the isthmus and genu of the human corpus callosum: a postmortem morphological study. *Brain*, *112*(3), 799-835.